Gold as a promoter for the activity of palladium in carbon-supported catalysts for the liquid phase oxidation of glyoxal to glyoxalic acid

Sophie Hermans and Michel Devillers*

Catholic University of Louvain, Unité de Chimie des Matériaux Inorganiques et Organiques, Place L. Pasteur 1/3, B-1348 Louvain-la-Neuve, Belgium

Received 10 August 2004; accepted 14 October 2004

Bimetallic Pd–Au/C catalysts were prepared by various methods, including deposition–precipitation. It was found that these catalysts are highly active for the selective oxidation of glyoxal into glyoxalic acid in aqueous phase, while the corresponding monometallics displayed no (in the case of Au/C) or very little (in the case of Pd/C) activity.

KEY WORDS: carbon; glyoxal; glyoxalic acid; gold; liquid phase; palladium; selective oxidation; supported catalysts.

1. Introduction

Since the precursor work by Haruta *et al.* gold has found a new surge of interest for catalytic applications [1–4]. It was found that gold supported on titania (or other similar inorganic oxides) could be an active catalyst for CO oxidation at low temperature, but under strict control of the Au particle size:only nanoparticulate gold displayed the desired activity [5,6]. This has been explained in various terms, including relativistic effects, differences of electron density and number of surface atoms (in low coordination number) in nano-sized objects, or increased support/particle interface [7]. Since these early reports, various researchers have found an activity for monometallic supported gold catalysts, in a variety of oxidation and hydrogenation reactions [3], including liquid phase applications [8]. In particular, the group of Prati *et al.* has demonstrated the ability of Au/C catalysts to oxidise diols [9,10], carbohydrates [11] and aldehydes [12]. However, most of these studies rely on the ability of Au to act as an active element by itself, and bimetallic catalysts including gold remain scarce. In particular, the bimetallic Pd–Au association has been given little attention until very recently. The use of Pd–Au/SiO_2 catalysts is a well-established commercial route for the synthesis of vinyl acetate by acetoxylation of ethylene since the 1960's, but it is still poorly understood [13]. In recent studies, it has been shown that the addition of gold to a supported Pd catalyst does not improve its performance in some cases [14], but it has also been reported that bimetallic Pd–Au catalysts supported on various substrates (such as silica, alumina, ceria, titania, carbon, zeolites, magnesium fluoride, niobium oxide, etc.) give rise to increased activity and/or selectivity when compared to their monometallic counterparts, and this for a wide variety of catalytic applications (hydrogenation of toluene, naphthalene, acetylene, 1,3-butadiene, or 2-hexyne; methanol or nitric oxide decomposition; hydrodechlorination; hydrodesulfurization; methylcyclopentane hydroconversion; trimerization of acetylene, etc.). However, only two papers deal with applications of Au–Pd catalysts in oxidation reactions: for CO [15] and ethanal oxidation [16].

In this paper, we wish to report the results of a study that was aimed at the preparation, characterisation, and use in liquid phase oxidation, of bimetallic Pd–Au/C catalysts. The reaction considered is the selective oxidation of glyoxal into glyoxalic acid, a transformation that finds its justification in the fact that glyoxalic acid is an important intermediate in the cosmetic and food industries, and in particular for the synthesis of vanillin [17]. Moreover, due to the variety of by-products that can be formed (oxalic and formic acids by over-oxidation; glycolic acid by Cannizzaro dismutation, see figure 1), subtle effects due to the nature of the catalyst, or its surface state, can easily be detected. The first report on the use of heterogeneous catalysts for this reaction, as an alternative for the industrial process using stoichiometric amounts of nitric acid, deals with monometallic noble metal carbon-supported materials [18]. Since then, we have shown that the addition of a promoter element such as bismuth or lead can improve drastically the catalyst' performance, but with a major drawback of Bi and Pb leaching in solution during reaction [19,20]. This limitation for promoted Pd/C catalysts has also been noted for another reaction catalysed in the aqueous phase: the selective oxidation of d-glucose into gluconic acid [21]. Hence there is scope for finding new catalyst formulations, that would be stable and highly performant for selective oxidations carried out in water, in

* To whom correspondence should be addressed.
E-mail: devillers@chim.ucl.ac.be

1011-372X/05/0100–0055/0

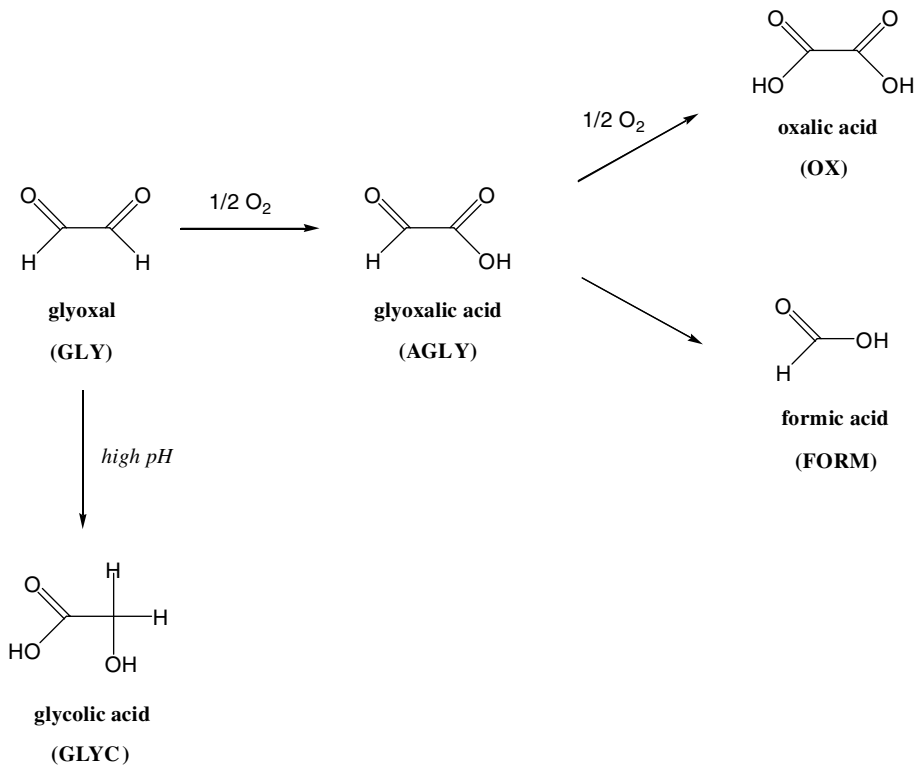

Figure 1. Possible by-products in the catalytic oxidation of glyoxal
(*Note*: the production of glycolic acid depends only on the pH by Cannizzaro dismutation and is thus truly homogeneous).

order to replace the current industrial options by environmentally-friendly and economically-viable alternatives.

2. Experimental

2.1. Catalysts preparation

Monometallic and bimetallic catalysts were prepared either from a commercial monometallic Pd(5 wt%)/C catalyst [Aldrich], or by incorporation of the metal precursor(s) on SX +active carbon supplied by NORIT (selected particles size = 50–100 μm, $S_{BET} \cong 800\ m^2/g$). The total metal loading obtained was about 5 wt% in the case of monometallic and 10 wt% in the case of bimetallic catalysts. The precursors used were $Pd(OAc)_2$ [Aldrich, 98%] or $PdCl_2$ [Aldrich, 99.9 + %] for palladium and $HAuCl_4 \cdot 3H_2O$ [Aldrich, 99.9 + %] for gold.

Three different methods for incorporation and activation of the metallic precursor(s) on the support were implemented:

(i) Deposition in *n*-heptane [21]: The chosen metallic precursor was sonicated for 30 min in *n*-heptane (100 mL) in the presence of the required amount of monometallic catalyst or SX + carbon support. The solvent was then slowly evaporated under reduced pressure at room temperature. The obtained fresh catalyst was subsequently activated at 500 °C for 18 h under nitrogen flux in a tubular oven. In the case of bimetallic catalysts prepared from SX + carbon, the two metallic precursors were deposited in turn following the same method, before activating only once the obtained M–M′/C (where M′ denotes the metal incorporated in second position) materials.

(ii) Precipitation–reduction as described by Prati *et al.* [9]: The gold precursor was dissolved in a minimum amount of water, by addition of HCl if necessary. The pH of the solution was adjusted at 10 by dropwise addition of a saturated solution of Na_2CO_3 [Aldrich, 99.5 + %]. This mixture was then added, while stirring, to a suspension of carbon (or monometallic commercial catalyst) in 100 mL water. After 1 h resting at room temperature, the catalyst was activated by dropwise addition of a formalin solution (HCHO 37%) [Aldrich]. The slurry was maintained at 70°C for 1 h, and the catalyst was then filtered and washed with 500 mL warm water in order to remove residual chlorine (the filtrate was tested for Cl^- with $AgNO_3$ [Aldrich, 99.995%]). The obtained catalyst was dried under vacuum at 80°C for 6 h.

(iii) Method described in a patent by Saito *et al.* [22]: The first metallic precursor was dissolved in water acidified with HCl. The carbon was added to this solution, which was then agitated for 6 h at room temperature. A solution containing the second metallic precursor was added dropwise, before

adding a 20 wt% solution of NaOH [Riedel-deHaën, 99%] in order to obtain a basic pH. The catalyst was activated by adding formalin, and keeping the slurry at 80°C for 1 h. The catalyst was recuperated by filtration, washed, and dried under vacuum at 80°C for 6 h.

2.2. Characterisation

The catalysts were characterised by X-ray powder diffraction (XRD), X-ray photoelectron spectroscopy (XPS) and Scanning Electron Microscopy (SEM) before and after use in catalytic tests:

2.2.1. XRD

The XRD analyses were performed with a D5000 SIEMENS diffractometer equipped with a copper source ($\lambda_{K\alpha} = 154.18$ pm). The samples were supported on quartz monocrystals. The phases detected were identified by reference to the JCPDS database.

2.2.2. XPS

The XPS measurements were carried out at room temperature on a SSI-X-probe (SSX-100/206) photoelectron spectrometer from Surface Science Instruments (USA) equipped with a monochromatized microfocus Al X-ray source (powered at 20 mA and 10 kV). The samples were stuck onto small troughs with double-sided adhesive tape, and then placed on an insulating home made ceramic carrousel (Macor® Switzerland), with the nickel grid, mentioned below, still grounded to the carrousel support, to avoid differential charging effects. The pressure in the analysis chamber was around 10^{-6} Pa. The angle between the surface normal and the axis of the analyser lens was 55°. The analysed area was approximately 1.4 mm^2 and the pass energy was set at 150 eV. In these conditions, the resolution determined by the full width at half maximum (FWHM) of the Au $4f_{7/2}$ peak was around 1.6 eV. A flood gun set at 8 eV and a Ni grid placed 3 mm above the sample surface were used for charge stabilisation. The quantification was based on the C_{1s}, Au_{4f}, Pd_{3d}, Cl_{2p} and Na_{1s} photopeaks. The energy calibration was done with reference to the peak Au $4f_{7/2}$ at 84 eV, and the binding energies were calculated with respect to the C–(C, H) component of the C_{1s} peak fixed at 284.8 eV. Data treatment was performed with the CasaXPS program (Casa Software Ltd, UK). The spectra were decomposed with the least squares fitting routine provided by the software with a Gaussian/Lorentzian (85/15) product function, after subtraction of a Shirley type baseline [23], and using the following constraints: for gold, intensity ratio (Au $4f_{7/2}$/Au $4f_{5/2}$) = 1.33, $\Delta = 3.67$ eV, fwhm ratio = 1; for palladium, intensity ratio (Pd $3d_{5/2}$/Pd $3d_{3/2}$) = 1.5, $\Delta = 5.26$ eV, fwhm ratio = 1; for chlorine, intensity ratio (Cl $2p_{3/2}$/Cl $2p_{1/2}$) = 2, $\Delta = 1.6$ eV, fwhm ratio = 1. Molar fractions were calculated using peak areas normalised on the basis of acquisition parameters and sensitivity factors provided by the manufacturer.

2.2.3. SEM

The SEM analyses were performed on a field effect gun digitan scanning electron microscope (DSM 982 Gemini from LEO), equipped with an energy dispersive X-ray system (EDAX Phoenix equipped with a CDU LEAP detector). The powder samples were pressed onto conducting double-face adhesive tape fixed onto 0.5″ aluminium specimen stubs from Agar Scientific.

2.3. Catalytic testing

The catalytic reaction was carried out in a double-walled glass reactor, allowing temperature control by water circulation in the outer compartment, equipped with a electronically-controlled HEIDOLPH 2051 stirrer, as described previously [19,20]. The pH of the reaction was continuously measured and controlled *via* a combined electrode BECKMAN 39843 connected to an automatic titration METROHM (718 STAT Titrino) device. The pH was fixed at 7.7 by addition of a solution of Na_2CO_3 0.5 mol/L [Aldrich] and the duration of the catalytic tests was 20 h, unless otherwise stated. The other experimental conditions used for catalytic testing are summarised in table 1.

At the end of the catalytic reaction, the catalyst was recuperated by filtration for characterisation, and the filtrate was analysed by HPLC and ICP. The reaction products were quantified by HPLC, using a Thermo Separation Products (TSP) chromatograph equipped with a Spectra system UV 6000LP detector, on a Bio Rad Aminex HPX-87H column. The column was heated at 60 °C, the injected volume was 20 μL, and the mobile phase was a 0.005 mol/L sulfuric acid solution [Riedel-de Haën] with a flux of 0.4 L/min. The products were detected at 230 nm after calibration with pure solutions of each different envisageable acid (see figure 1). The results are expressed in terms of yield in each different product (Y, %), conversion (X, %), and selectivity (S, %), as defined below:

$$Y = C_{\text{product}}/C_{\text{glyoxal at } t=0} \quad (1)$$

where C = concentration

$$X_{GLY} = Y_{AGLY} + Y_{OX} + Y_{GLYC} + (Y_{FORM})/2 \quad (2)$$

Table 1
Experimental conditions used for catalytic testing

Parameter	Value
Starting volume of glyoxal solution (0.1 mol/L)	400 mL
Temperature	38 °C
Stirring rate	1000 rpm
pH	7.7
Air flow (oxidant)	0.4 L/min
Mass of catalyst	100 mg

$$S_{AGLY} = (Y_{AGLY}/X_{GLY}) \cdot 100 \quad (3)$$

However, as the Cannizzaro dismutation responsible for the production of glycolic acid depends only on the pH and is totally independent of the catalyst, we also define the corrected conversion X^* and corrected selectivity S^* as follows:

$$X^* = Y_{AGLY} + Y_{OX} + (Y_{FORM})/2 \quad (4)$$

$$S^*_{AGLY} = (Y_{AGLY}/X^*) \cdot 100 \quad (5)$$

The occurrence of metal leaching (if any) was determined by ICP analysis of the reaction filtrate. These analyses were carried out on a Perkin–Elmer Optima 3000 SC device, equipped with a Segmented-array Charge Coupled Device detector. The wavelengths used for analysis were 340.458 nm for Pd and 242.795 nm for Au. The plasma conditions were as follows:RF power: 1300 W, Ar 17 L/min, sample flow 1 mL/min.

3. Results and discussion

Various monometallic M(5 wt%)/C and bimetallic M–M′(10 wt%)/C (where M′ denotes the metal incorporated in second position) catalysts have been prepared by three different methods (see Experimental for details):(i) deposition of metal(s) precursor(s) by sonication in *n*-heptane followed by thermal activation [21], (ii) precipitation–reduction as described by Prati *et al.* [9], or (iii) the method described in a patent by Saito *et al.* [22]. The two last methods involve chemical activation with formalin. The catalysts obtained were tested for the catalytic oxidation of glyoxal into glyoxalic acid in aqueous phase, and the results obtained will be discussed below for each different category of catalysts that might be taken into consideration.

3.1. Monometallic catalysts

The uppermost part of table 2 shows the catalytic performance obtained with the monometallic M(5 wt%)/C catalysts after 20 h. The Pd/C catalysts displayed only moderate activity, and the Au/C materials were inactive for the oxidation reaction. These will be used as 'references' for discussing the results presented in the following sections. The fact that the monometallic Au/C catalysts were inactive is slightly surprising, given that these were found to be active in other liquid-phase selective oxidations [8,9].

3.2. Bimetallic catalyst prepared by dispersion in n-heptane

The results obtained with a bimetallic Pd–Au/C catalyst prepared by dispersion in *n*-heptane and thermal activation, are also displayed in table 2. It is obvious that this catalyst was inactive, and even more, that it was less efficient than the corresponding monometallic Pd/C. This method of preparation leads thus to a form of gold that is detrimental to the catalytic activity of Pd. This could be due to the presence of residual chlorine originating from the gold precursor and/or incomplete reduction during the thermal activation step.

3.3. Bimetallic Pd–Au/C catalysts prepared by precipitation–reduction as described by Prati et al. [9] and/or by the method described in a patent by Saito et al. [22] (wt. ratio Pd:Au = 1)

The catalytic performance of the bimetallic Pd–Au/C (or Au–Pd/C) catalysts prepared by precipitation–reduction as described by Prati *et al.* [9] or by the method described in a patent by Saito *et al.* [22] (or a combination of the two) are presented in the lower part of table 2. All these catalysts were very active and

Table 2
Catalytic performance of the monometallic M/C and bimetallic M–M′/C (wt. ratio M:M′ = 1) catalysts for t = 20 h (catalytic testing with m_{CAT} = 100 mg, com = commercial). Some values have been averaged over several catalytic tests

Catalyst	Metal 1	Precursor 2	Prep. method	Y_{AGLY} (%)	Y_{OX} (%)	Y_{FORM} (%)	X^* (%)	S^* (%)
Pd/C com [a]	–	–	–	9.6	1.1	0.0	10.7	90
Pd/C [a]	$Pd(OAc)_2$	–	heptane	10.3	1.1	0.0	11.4	91
Au/C [a]	$HAuCl_4$	–	heptane	0.0	0.0	0.0	0.0	–
Au/C	$HAuCl_4$	–	Prati	0.8	0.3	0.0	1.0	75
Au/C [a,b]	$HAuCl_4$	–	Prati	0.9	0.3	0.8	1.6	61
Pd–Au/C [a]	$Pd(OAc)_2$	$HAuCl_4$	heptane	2.2	–	–	2.2	100
Au–Pd/C [a]	$HAuCl_4$	$PdCl_2$	Saito	4.1	0.3	0.0	4.4	93
Au–Pd/C	Au/C Prati	$PdCl_2$	Saito	14.0	2.0	5.9	18.9	74
Pd–Au/C	Pd/C com	$HAuCl_4$	Saito	17.4	4.0	7.2	25.0	70
Pd–Au/C	Pd/C com	$HAuCl_4$	Prati	22.2	5.9	10.7	33.5	66
Au–Pd/C	Au/C Prati	$PdCl_2$	Prati	22.2	8.2	13.0	36.9	61

[a]pH control during catalytic reaction by addition of a 2 wt% solution of NaOH.
[b]this catalyst contains only 1 wt.% metal loading.

selective, and more so than the Pd/C or Au/C 'references' (compare with upper part of the table). This means that under these preparative conditions, gold can play a promoter role for the activity of palladium. This was further demonstrated by the catalysts prepared by simply adding gold onto pre-formed monometallic commercial Pd/C catalysts. The Pd–Au/C catalysts prepared following Prati's method, from a pre-made commercial Pd/C catalyst or from SX + carbon and $PdCl_2$, were the most active (in terms of yield in glyoxalic acid, the desired product). It is outstanding that these results are the best ever obtained for this reaction, when comparing with our previous studies with Pd–Bi/C catalysts [19,20], which include comparison with the literature [18] and a commercial trimetallic catalyst from Degussa. The Pd–Au/C catalysts prepared following Saito's method are not as active, but are more selective, due to lower yields in formic and oxalic acids.

3.4. Influence of the Pd/Au wt. ratio in bimetallic Pd–Au/C catalysts

Table 3 presents the catalytic results obtained with bimetallic Pd–Au/C catalysts prepared by precipitation–reduction as described by Prati *et al.* [9] from the monometallic commercial Pd(5 wt%)/C catalyst and $HAuCl_4$, and in which the weight ratio Pd:Au was varied (i.e. the amount of gold added onto the Pd/C catalyst was different in each case). Table 3 also contains the results obtained with the monometallic Pd/C and Au/C catalysts, for comparison. It is striking that the results obtained were more or less always the same: the yield in glyoxalic acid is about 20% regardless of the composition, and always much higher than the yields obtained with the monometallic counterparts. The selectivity, however, was slightly variable, with a decrease in the production of oxalic acid when the amount of gold added was higher, yielding optimised values of corrected selectivity (S^*) at low Pd/Au ratios. In order to draw comparisons in a more accurate manner, the catalytic results were normalised with respect to either the mass of Pd, the mass of Au, or the total mass of metal (Pd + Au) in the catalysts (table 4). The yield in glyoxalic acid per mg of Pd was found to be constant and ca. 4% mg^{-1} regardless of the amount of gold present in the catalyst: adding only a small amount of gold on a pre-formed Pd/C catalyst enhances thus its catalytic activity dramatically.

3.5. Activity as a function of time

Because of the general scheme for glyoxal oxidation, involving consecutive and parallel reactions (see figure 1), it is important to determine t_{max}, the optimal time after which the maximum yield in glyoxalic acid is obtained before being over-oxidised to oxalic acid (figure 2). The activity of the Pd–Au/C catalysts was studied in function of time by continuous sampling (by taking 0.5 mL aliquots every hour) of the reaction mixture as a function of time. Figure 3 shows an example of kinetic plot obtained (these results include a correction for the volume variations induced by sampling). The other catalysts investigated as a function of time gave very similar pictures. It can be concluded from figure 3 that t_{max} for Pd–Au/C catalysts is ca. 24 h, a value which is very similar to t_{max} for Pd–Bi/C catalysts in the same reaction [19].

Table 4
Normalised (with respect to either the mass of Pd, the mass of Au, or the total mass of metal (Pd + Au) in the catalyst) catalytic performance of the bimetallic Pd–Au/C catalysts, with variable wt. ratio Pd:Au, prepared by precipitation–reduction as described by Prati *et al.* [9] from the monometallic commercial Pd(5 wt%)/C catalyst and $HAuCl_4$ (catalytic testing with m_{CAT} = 100 mg, t = 20 h)

Pd/Au (wt. ratio)	Y_{AGLY}/mPd (% mg^{-1})	Y_{AGLY}/mAu (% mg^{-1})	Y_{AGLY}/mMetal (% mg^{-1})
Au/C 5%	0.0	0.2	0.2
0.3	4.1	1.4	1.0
0.5	5.0	2.7	1.7
1	4.6	4.6	2.3
2	4.2	7.1	2.7
3	4.8	14.7	3.6
Pd/C 5%	1.9	0.0	1.9

Table 3
Catalytic performance of the bimetallic Pd–Au/C catalysts, with variable wt. ratio Pd:Au, prepared by precipitation–reduction as described by Prati *et al.* [9] from the monometallic commercial Pd(5 wt%)/C catalyst and $HAuCl_4$ (catalytic testing with m_{CAT} = 100 mg, t = 20 h). The values presented have been averaged over several catalytic tests

Pd/Au (wt. ratio)	Total metal loading in the catalyst (wt.%)	Y_{AGLY} (%)	Y_{OX} (%)	Y_{FORM} (%)	X^* (%)	S^* (%)
Au/C Prati	5.0	0.8	0.3	0.0	1.0	75
0.3	17.3	17.8	3.5	6.9	24.8	72
0.5	13.1	22.9	7.00	7.7	33.6	68
1	9.6	22.2	5.9	10.7	33.5	66
2	7.8	20.7	6.1	11.4	32.6	64
3	6.5	23.5	10.0	9.5	38.3	62
Pd/C commercial	5.0	9.6	1.1	0.0	10.7	90

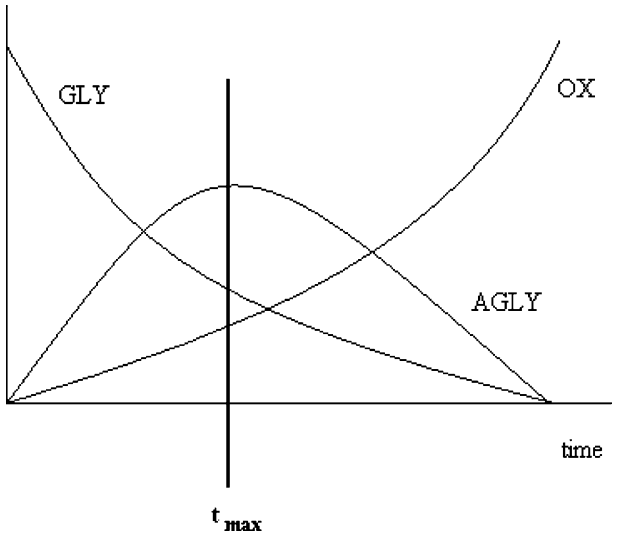

Figure 2. Schematic kinetic plot showing how we define t_{max}.

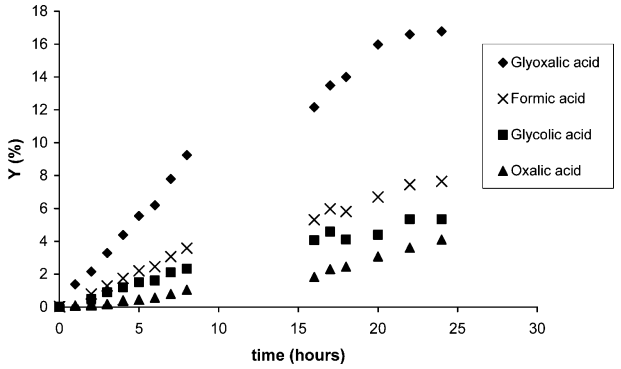

Figure 3. Catalytic activity as a function of time for a Pd–Au/C catalyst with Pd:Au wt. ratio = 0.5. prepared by precipitation–reduction as described by Prati *et al*. [9] from the monometallic commercial Pd(5 wt%)/C catalyst and $HAuCl_4$ (catalytic testing with m_{CAT} = 100 mg).

3.6. ICP

The filtrates of catalytic reactions were analysed by ICP in order to detect any trace of metal(s) that might be present in solution after test. In all the reaction mixtures analysed, no amount of either palladium or gold superior to 50 ppb was detected. This means that the Pd–Au/C catalysts are much more robust than the Pd–Bi/C or Pd–Pb/C materials, where the promoter element (Pb or Bi) leached could easily be detected by atomic absorption spectrometry.

3.7. Characterisation

The catalysts before (and sometimes after) use in catalytic tests were characterised by XRD, XPS and SEM. The results obtained with each different technique are discussed below.

3.7.1. XRD

The various monometallic and bimetallic catalysts described in this study were characterised by XRD only before their use in catalytic tests. Gold (metallic phase) was detected in all Au/C or Pd–Au/C catalysts, while palladium could not be observed in the catalysts originating from commercial ones. This could be due to the very high dispersions (hence small metallic particles) in the starting commercial materials. When comparing the catalysts prepared by dispersion in *n*-heptane and thermal activation with those activated by formalin (the so-called 'Prati' or 'Saito' methods), it is observed that both metals (Au + Pd) are detected in the former case, while only Au is detected in all the formalin-activated catalysts (indicating that very high Pd dispersions are also obtained in the latter case). In the case of the Pd–Au catalyst prepared in heptane, the presence of Pd_x Au_y alloys is suspected, because of the presence in the diffractogram of additional peaks that are intermediate between pure Au and pure Pd (figure 4 (a)). This is in agreement with the phase diagram for this bimetallic combination, which shows that gold is mostly miscible with Pd in the whole compositional range [24]. Moreover, when comparing the peaks ascribed to Au for the various catalysts prepared by different methods, an effect of peak widening was observed (see figure 4(b)). This means that the gold particles obtained *via* the chemical reduction route were smaller than with the heptane/thermal route. This was further confirmed by SEM characterisation (see below).

3.7.2. XPS

The results of XPS characterisation, before and after catalytic testing, for the monometallic and bimetallic catalysts reported in this paper are presented in table 5. The detailed analysis of these numbers, in comparison with values calculated on the basis of bulk compositions, brings about the following comments:

(a) *Au/C ratios*: The experimental values are in general higher than the calculated values, which indicates a good dispersion of gold in our catalysts. However, this observation is not generalised and the differences between experimental and calculated values are not important. The comparison between the XPS results for catalysts prepared by the 'heptane' method with those prepared by the 'Prati' method does not reveal any clear trend: for example the Au/C ratios obtained for the two monometallic catalysts are exactly the same (it should also be noted that the Au/C ratios for the monometallic catalysts were really small, indicating a low dispersion of gold when present alone). After test, the experimental Au/C ratios show a tendency to rise.

(b) *Pd/C ratios*: The values of experimental Pd/C ratios are very large (and unprecedented, see ref. [19]), especially for the catalysts activated chemically, and exceed by far the calculated values, demonstrating

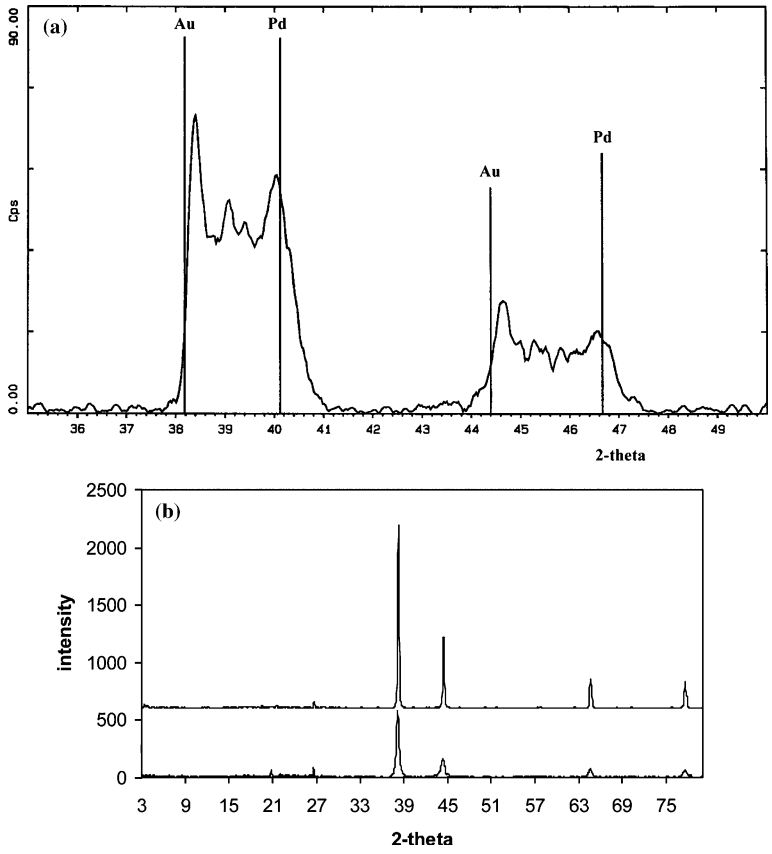

Figure 4. (a) Expansion of the zone of interest in the XRD diffractogram obtained for the Pd–Au/C catalyst prepared by dispersion in *n*-heptane (the vertical lines are the theoretical peaks for pure Au or Pd), and (b) comparison between the XRD diffractograms obtained for Au/C catalysts prepared by dispersion in *n*-heptane and thermal activation (top) and by chemical reduction with formalin (so-called 'Prati' method) (bottom).

that the dispersion of palladium must be really high at the surface of these catalysts. After test, the trend is also towards an increase for the Pd/C ratios.

(c) *Au/Pd ratios*: Given the tendencies described in the preceeding paragraphs, the Au/Pd experimental ratios are inferior to the calculated values in the case of the Pd–Au/C catalysts. After catalyst usage, the Au/Pd ratios seem to stay more or less constant.

(d) *Cl and Na*: All catalysts prepared from chlorinated precursors still contained residual chlorine, despite careful washings (and Ag^+ testing in the filtrates). Moreover, the amount of chlorine contamination does not really diminish after test. We also observed the presence of sodium in all the catalysts derived from commercial ones, and in most catalysts after use.

The oxidation state of gold and palladium seemed mainly to be zero (i.e. metallic gold and palladium) at the surface of our mono- or bimetallic catalysts, from the values of binding energies that were found to vary very little from 83.8 to 84.3 eV for the Au $4f_{7/2}$ peaks, and between 335.2 and 335.8 eV for the Pd $3d_{5/2}$ peaks. In all cases, the presence in our catalysts of small amounts of oxide of either metals could not be ruled out. No major difference in terms of oxidation states was observed between the samples before and after use in catalytic tests, and between the samples prepared by the different methods.

3.7.3. SEM

Several representative monometallic Au/C or bimetallic Pd–Au/C catalysts were examined by SEM coupled with elemental analysis by EDXS. In agreement with XPS characterisation, the monometallic Au/C catalysts showed supported metallic particles that were on average larger than in bimetallic catalysts (explaining the smaller values of Au/C atomic ratios in XPS). In order to compare the preparation methods, histograms of particle size distribution were constructed for two monometallic Au/C catalysts prepared by (i) dispersion in *n*-heptane and (ii) precipitation–reduction (Prati's method). This is shown in figure 5. It gave an average particle size of 89 nm for the catalyst prepared by deposition in heptane, and of 77 nm for the catalyst prepared by precipitation–reduction, confirming the differences also observed by XRD. For gold-based catalysts, these values of particle sizes are quite big, which might explain the non-activity of our Au/C materials. In the case of the bimetallic Pd–Au/C catalysts, the pictures

Table 5
Results of XPS characterisation (atomic intensity ratios) for monometallic and bimetallic catalysts prepared by the various methods reported in this paper: heptane = deposition in *n*-heptane and thermal activation [21], Prati = precipitation–reduction as described by Prati *et al.* [9], and Saito = method described in a patent by Saito *et al.* [22] (exp. = experimental values, calc. = values calculated on the basis of bulk compositions, com = commercial)

Catalyst	Loading M/M′ (wt%)	Au/C (x100)		Pd/C (x100)		Au/Pd	
		calc.	exp.	calc.	exp.	calc.	exp.
Au/C heptane	5	0.32	0.17	–	–	–	–
after test			0.17	–	–	–	–
Au/C Prati	5	0.32	0.16	–	–	–	–
after test			0.21	–	–	–	–
Pd–Au/C heptane	5/5	0.34	0.46	0.63	1.00	0.54	0.46
after test			0.73		1.30		0.56
Au–Pd/C Saito	5/5	0.34	0.14	0.63	0.51	0.54	0.27
after test			0.15		3.81		0.04
Pd(com)–Au(Saito)/C	4.8/4.8	0.32	1.25	0.60	2.78	0.54	0.45
Au(Prati)–Pd(Saito)/C	4.8/4.8	0.32	0.21	0.60	2.43	0.54	0.09
after test		0.32	0.24	0.60	2.56	0.54	0.09
Au–Pd/C Prati	4.8/4.8	0.32	0.41	0.60	5.71	0.54	0.07
after test			0.21		4.48		0.05
Pd(com)–Au/C Prati	4.8/4.8	0.32	0.79	0.60	1.86	0.54	0.43
after test			0.96		2.35		0.41
Pd(com)–Au/C Prati	4.6/8.5	0.60	1.46	0.60	2.52	0.99	0.58
after test		0.60	1.39	0.60	2.76	0.99	0.504
Pd(com)–Au/C Prati	4.9/2.9	0.19	0.66	0.60	2.34	0.32	0.28
after test		0.19	0.63	0.60	2.39	0.32	0.26
Pd(com)–Au/C Prati	4.9/1.6	0.10	0.67	0.59	2.7	0.18	0.25

obtained by SEM showed a homogeneous distribution of small nanoparticles, which sizes were on average comprised between 10 and 50 nm. Figure 6 shows a representative example of SEM image obtained for an active catalyst. The EDXS analysis of such a zone gave the signals corresponding to the carbon support, gold and palladium, as expected figure 7). However, it was very difficult to assess whether these nanoparticles were truly bimetallic, or whether they contained only one of the two metals (most probably Au) with a layer of the other (Pd) very well dispersed underneath, as would be consistent with DRX and XPS analyses. The influence of the preparation method on the microstructure of bimetallic Pd–Au/C catalysts could not clearly be demonstrated by SEM either, although small differences in particles sizes and shapes were noted, but these would not be sufficient to explain the drastic differences observed in terms of catalytic activity.

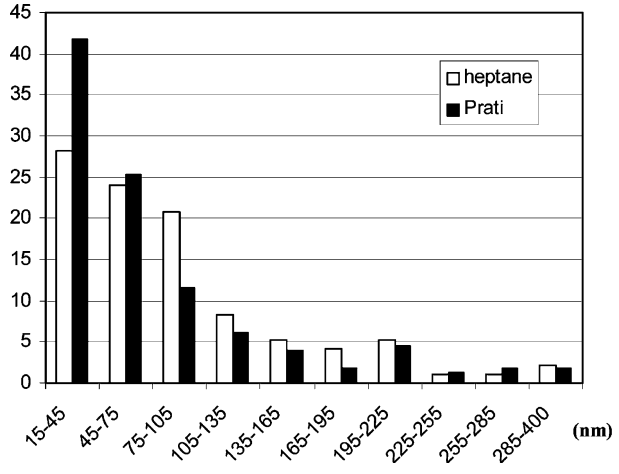

Figure 5. Histogram of particle size distributions derived from SEM analysis of monometallic Au/C catalysts prepared by two different methods (the particle sizes given on the *x*-axis are in nm).

3.8. General discussion

In order to compare the catalytic activity of the Pd–Au/C catalysts described here with values from the literature, it is necessary to consider the yields in glyoxalic acid at t_{max}, and to normalise them with respect to the amount of active metal in the catalyst. This has been done for a range of catalysts, arising from this paper and from the literature, and is shown in table 6. The values obtained for the Pd–Au/C catalysts were ca. 1.5-times higher than for the Bi–Pd/C catalysts, which were the most active so far for this reaction, under the same reaction conditions. The promoting ability of gold for palladium in this reaction is thus higher than that of bismuth in terms of yield. The reaction kinetics are very similar (with $t_{max} \cong 24$ h), but the stability is very

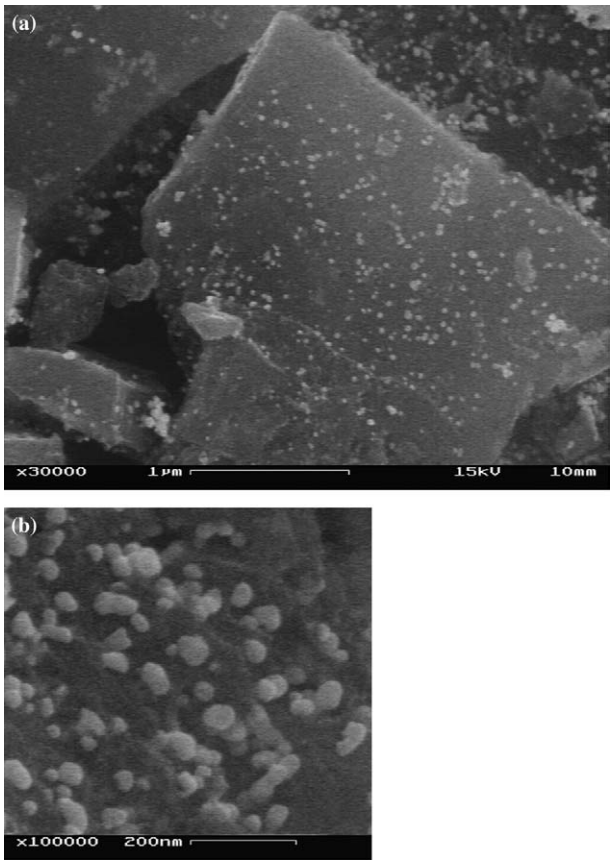

Figure 6. Typical SEM picture for an active Pd–Au/C bimetallic catalyst (a) at low magification (30,000×), showing the homogeneous distribution of nanoparticles on the support and (b) at high magnification (100,000×), showing the particle sizes.

different: while Bi was found to leach in significant amounts, no detectable amount of gold was found in solution after catalytic reaction (the detection limit being 10 ppb for Au). In consequence, the bimetallic Pd–Au combination constitutes an interesting alternative for Bi–Pd, with good properties of activity and robustness. It is also more active than a trimetallic commercial formulation from Degussa. In the literature, the bimetallic Au–Pd system has been used mainly for hydrogenation, decomposition or hydrodechlorination/hydrodesulfurization, as mentioned in the introduction. This is thus one of the few examples of Au–Pd catalysts used successfully in oxidation reactions.

The exact mechanism of gold promotion still remains to be elucidated, but the answer lies perhaps in a dispersion effect (as the Pd/C ratios measured by XPS at the surface of the active Pd–Au/C catalysts were particularly high). Geometric or electronic effects cannot be ruled out, even if the bimetallic nature of the particles could not be confirmed:a decoration of the Pd phase by Au could lead to a phenomenon of site blocking (geometric effect), while the presence of an interface between Au and Pd could lead to subtle electronic effects. The differences in catalytic activity for the catalysts prepared by the different methods may be related to particle sizes and Pd dispersion:the catalysts prepared by dispersion in heptane present larger Au and Pd particles, while those activated chemically display much smaller Pd particles (and higher XPS Pd/C ratios), and relatively smaller Au particles too. In addition, the 'Prati' method leads to the smallest Au particles and the most active catalysts. The promoting effect of gold might thus also be associated with the size of the supported particles, as was noted for its catalytic activity, which is inversely proportional to the particle size for Au, in other reactions [9]. If the Au particle size could be decreased further, one could expect a further enhancement of the catalytic activity of our Pd–Au/C catalysts. However, the risk of other compounds, like

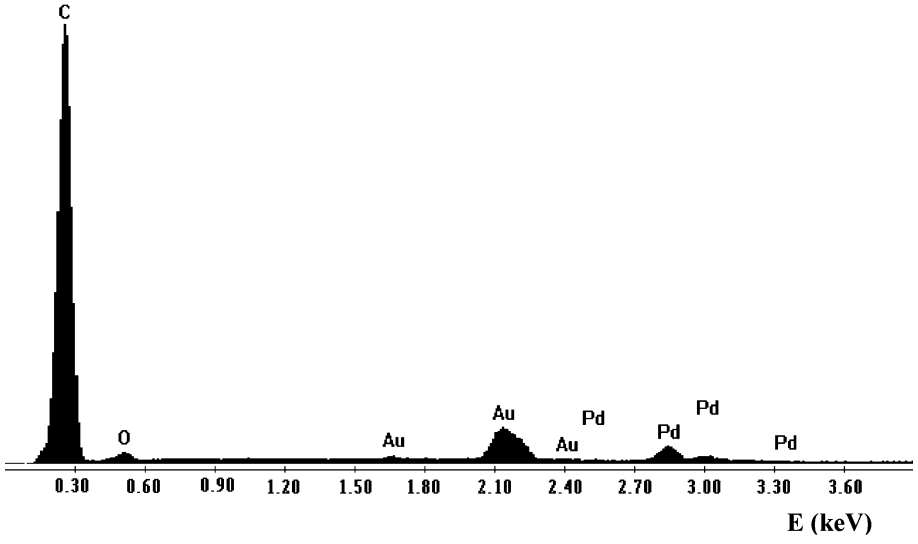

Figure 7. EDXS spectrum associated with the pictures shown in figure 6.

Table 6
Comparison of normalised catalysts performance in this work, in our previous publications and in the literature [18,19]

Catalyst	t_{max}(h)	$(Y_{AGLY})_{max}/m$Pd, Pt (mol/g)
In this study:		
Pt/C commercial	>20	0.93
Pd/C commercial	>9	0.17
Pd–Au/C	24	1.6–2.0
Previously:		
Pt/C [18]	1.5	0.55
Pd/C [18]	–	0.38
Bi–Pd/C [19]	24	1.22
Bi–Pd–Pt/C Degussa [19]	8	0.78

formic acid, becoming the major products of the reaction should not be underestimated [25]. The key-point here is to keep the selectivity to glyoxalic acid as high as possible, for the shortest possible t_{max}.

4. Conclusion

In this paper, we have shown that gold can have a clear promoting effect for the activity of palladium in the reaction of glyoxal selective oxidation carried out in water. The monometallic Au/C catalysts were inactive, but the bimetallic Pd–Au/C catalysts were at least twice more active than the best Pd/C materials. Moreover, the Pd–Au catalysts were more active than the Pd–Bi/C or Pd–Pb/C catalysts that gave the best performance so far for this reaction. In addition, no metal leaching could be detected in the reaction mixtures, meaning that these Pd–Au catalysts are remarkably stable in very demanding conditions (in the presence of water and oxygen, with reactants that possess chelating properties), a fact that was the limitation of the Pd–Bi(Pb) systems. These Pd–Au/C catalysts represent thus a viable alternative for this reaction, and the promoting ability of gold might be extendable to other liquid phase oxidations.

Acknowledgments

The authors gratefully acknowledge the firm NORIT for supplying the carbon support, and the Belgian National Fund for Scientific Research (F.N.R.S.) for funding (Research Fellowship for S.H. as 'F.N.R.S. Postdoctoral Researcher'). We are also immensely grateful to (the late) Prof. P. Grange (head of the 'Unité de catalyse et de chimie des matériaux divisés', UCL) for access to XRD and XPS, and to E. Ferain for assistance during SEM manipulations. We also wish to thank G. Ploegaerts and V. Dubois (Institut Meurice, Bruxelles) for the ICP analyses. Many thanks also go to S. Vanderheyden and J.-F. Statsijns for technical support and to M. Genet for useful discussions regarding XPS characterisation.

References

[1] D. Thompson, Gold Bull. 31 (1998) 111.
[2] D. Thompson, Gold Bull. 32 (1999) 12.
[3] G.C. Bond and D.T. Thompson, Catal. Rev.–Sci. Eng. 41 (1999) 319.
[4] A. Haruta, Chem. Rec. 3 (2003) 75.
[5] D. Cunningham, S. Tsubota, N. Kamijo and M. Haruta, Res. Chem. Interm. 19 (1993) 1.
[6] S.D. Lin, M. Bollinger and M.A. Vannice, Catal. Lett. 17 (1993) 245.
[7] M. Haruta, S. Tsubota, A. Ueda and H. Sakurai, Stud. Surf. Sci. Catal. 77 (1993) 45.
[8] L. Prati and G. Martra, Gold Bull. 32 (1999) 96.
[9] L. Prati and M. Rossi, J. Catal. 176 (1998) 552.
[10] L. Prati and M. Rossi, Stud. Surf. Sci. Catal. 110 (1997) 509.
[11] S. Biella, L. Prati and M. Rossi, J. Catal. 206 (2002) 242.
[12] S. Biella, L. Prati and M. Rossi, J. Mol. Catal. A: Chem. 197 (2003) 207.
[13] N. Macleod, J.M. Keel and R.M. Lambert, Appl. Catal. A: Gen. 261 (2004) 37.
[14] see for example: P. Canton, F. Menegazzo, M. Signoretto, F. Pinna, P. Riello, A. Benedetti and N. Pernicone, Stud. Surf. Sci. Catal. 143 (2002) 1011.
[15] L. Guczi, A. Beck, A. Horvath, Z. Koppany, G. Stefler, K. Frey, I. Sajo, O. Geszti, D. Bazin and J. Lynch, J. Mol. Catal. A: Chem. 204 (2003) 545.
[16] R. Brayner, D.D. Cunha and F. Bozon-Verduraz, Catal. Today 78 (2003) 419.
[17] G. Mattioda and Y. Christidis *Ullmann's Encyclopedia of Industrial Chemistry,* 5th ed., Vol. A 12 (VCH, Weinheim, 1989) p. 495.
[18] P. Gallezot, R. de Mésanstourne, Y. Christidis, G. Mattioda and A. Schouteeten, J. Catal. 133 (1992) 479.
[19] F. Alardin, P. Ruiz, B. Delmon and M. Devillers, Appl. Catal. A: Gen. 215 (2001) 125.
[20] F. Alardin, B. Delmon, P. Ruiz and M. Devillers, Catal. Today 61 (2000) 255.
[21] M. Wenkin, P. Ruiz, B. Delmon and M. Devillers, J. Mol. Catal. A:Chem. 180 (2002) 141.
[22] H. Saito, S. Ohnaka and S. Fukuda, European Patent no. 0 142 725 B1, (1987).
[23] D.A. Shirley, Phys. Rev. B 5 (1972) 4709.
[24] H. Okamoto and T.B. Massalski *Binary Alloy Phase Diagrams,* Vol. 1–2 (American Society for Metals, 1986) pp. 295.
[25] H. Berndt, A. Martin, I. Pitsch, U. Prüsse and K.-D. Vorlop, Catal. Today 91 (2004) 191.